Published in final edited form as:
J Am Chem Soc. 2011 May 25; 133(20): 7916–7925. doi:10.1021/ja201249c.

Hydrogen-Bonding Catalysis and Inhibition by Simple Solvents in the Stereoselective Kinetic Epoxide-Opening Spirocyclization of Glycal Epoxides to Form Spiroketals

Jacqueline M. Wurst[†], **Guodong Liu**[‡], and **Derek S. Tan**[*,†,‡]

[†]Tri-Institutional Training Program in Chemical Biology, Memorial Sloan–Kettering Cancer Center, 1275 York Avenue, Box 422, New York, New York 10065, United States

[‡]Molecular Pharmacology & Chemistry Program, and Tri-Institutional Research Program, Memorial Sloan–Kettering Cancer Center, 1275 York Avenue, Box 422, New York, New York 10065, United States

Abstract

Mechanistic investigations of a MeOH-induced kinetic epoxide-opening spirocyclization of glycal epoxides have revealed dramatic, specific roles for simple solvents in hydrogen-bonding catalysis of this reaction to form spiroketal products stereoselectively with inversion of configuration at the anomeric carbon. A series of electronically-tuned C1-aryl glycal epoxides was used to study the mechanism of this reaction based on differential reaction rates and inherent preferences for S_N2 versus S_N1 reaction manifolds. Hammett analysis of reaction kinetics with these substrates is consistent with an S_N2 or S_N2-like mechanism ($\rho = -1.3$ vs. $\rho = -5.1$ for corresponding S_N1 reactions of these substrates). Notably, the spirocyclization reaction is second-order dependent on MeOH and the glycal ring oxygen is required for second-order MeOH catalysis. However, acetone cosolvent is a first-order inhibitor of the reaction. A transition state consistent with the experimental data is proposed in which one equivalent of MeOH activates the epoxide electrophile via a hydrogen bond while a second equivalent of MeOH chelates the sidechain nucleophile and glycal ring oxygen. A paradoxical previous observation that decreased MeOH concentration leads to increased competing intermolecular methyl glycoside formation is resolved by the finding that this side reaction is only first-order dependent on MeOH. This study highlights the unusual abilities of simple solvents to act as hydrogen-bonding catalysts and inhibitors in epoxide-opening reactions, providing both stereoselectivity and discrimination between competing reaction manifolds. This spirocyclization reaction provides efficient, stereocontrolled access to spiroketals that are key structural motifs in natural products.

INTRODUCTION

Catalysts that exploit hydrogen bonds to accelerate organic reactions are powerful complements to Lewis acids. Mild and environmentally benign, Brønsted acids are often effective catalysts because their weak interactions with substrates afford low product inhibition and high turnover.[1] Indeed, the seminal disclosure by Wassermann on the acceleration of Diels–Alder cycloadditions by phenol and substituted acetic acids preceded the first report of Lewis acid catalysis of this reaction by nearly two decades.[2] However,

[*]AUTHOR INFORMATION: Corresponding Author: tand@mskcc.org.

ASSOCIATED CONTENT

Supporting Information. Complete experimental procedures, characterization data for all new compounds, and kinetic data in tabular format. This material is available free of charge via the Internet at http://pubs.acs.org.

hydrogen-bonding catalysis did not recapture scientific interest until the mid-1980s, when Hine demonstrated the power of cooperative hydrogen-bonding interactions in the epoxide opening of phenyl glycidyl ether, in which 1,8-biphenylene diol provided a 600-fold rate increase compared to a monoprotic acid of the same strength.[3] Related bidentate catalysis by proximal tyrosine residues has also been observed in epoxide hydrolase enzymes.[4] These studies set the stage for the more recent development of other epoxide-opening reactions that are catalyzed by hydrogen-bonding interactions with hydroxyl functionalities.

We have previously reported a novel MeOH-induced kinetic epoxide-opening spirocyclization of glycal epoxides to form spiroketal products stereoselectively with inversion of configuration at the anomeric carbon (Figure 1).[5,6] A complementary Ti(O*i*-Pr)$_4$-catalyzed spirocyclization reaction provides the C1-epimeric spiroketals with retention of configuration at the anomeric carbon.[7] These reactions afford stereocontrolled access to spiroketals, independent of thermodynamic considerations that govern classical approaches to these structures.[8]

We have proposed that the MeOH-induced epoxide-opening spirocyclization proceeds via hydrogen-bonding catalysis.[5] This hypothesis was based on several observations: (1) Polar aprotic solvents do not induce spirocyclization, suggesting that the reaction is not driven simply by solvent polarity effects. (2) A methyl glycoside side product, which results from competing intermolecular epoxide opening with MeOH, is not converted to the spiroketal product upon reexposure to reaction conditions, eliminating it as a potential intermediate in mechanisms involving nucleophilic catalysis by MeOH. (3) Subjection of a thermodynamically-favored retention product (**4**) to the reaction conditions does not afford the inversion product (**3**), indicating that the MeOH-induced spirocyclization is under kinetic control.[5]

Subsequently, related epoxide-opening reactions have been reported to be catalyzed by water, methanol, and other simple alcohols, and similarly proposed to proceed via hydrogen-bonding catalysis. Jamison and coworkers have reported second-order catalysis by water in their landmark studies of regioselective epoxide-opening cascades to form ladder polyethers.[9] Williams and coworkers have provided computational support for hydrogen-bonding catalysis at the distal epoxide in their intriguing work on spirodiepoxide-opening reactions.[10] To date, however, the role of hydrogen-bonding catalysis in epoxide-opening spirocyclizations of glycal epoxides, and the critical and distinctive impact upon stereoselectivity in this reaction, has not been studied in detail. Outstanding questions also remain regarding the possible role of acetone, a residual cosolvent from the initial glycal epoxidation with dimethyldioxirane, and the paradoxical observation that decreased MeOH concentrations lead to increased competing intermolecular methyl glycoside formation.

Herein, we report our detailed mechanistic studies of this reaction using kinetic analyses of a series of electronically-tuned glycal epoxide substrates. Experimental evidence is provided for stereoselective formation of inversion products **3** via an S_N2 or S_N2-like reaction manifold, rather than an alternative S_N1 mechanism. We have also investigated the temperature dependence of the reaction, determined the kinetic order of MeOH in the transition state, identified the acetone cosolvent as an inhibitor of the reaction, and unraveled the paradox regarding competing intermolecular methyl glycoside formation. A transition state structure is proposed based on these experimental results.

RESULTS AND DISCUSSION

Our glycal epoxide substrates are structurally and electronically distinct from the 1,2-dialkyl epoxide and spirodiepoxide substrates studied previously by the Jamison and Williams

groups.[9,10] In particular, the observed stereoselectivity for inversion of configuration at the anomeric carbon may be attributed to either of two possible reaction mechanisms (Figure 2). An S_N2 reaction manifold (pathway A) would require sufficient hydrogen-bonding activation of the epoxide electrophile to induce nucleophilic substitution by the sidechain hydroxyl group without formation of a discrete oxocarbenium intermediate, which might lead to reduced stereoselectivity. Alternatively, an S_N1 mechanism (pathway B) might still afford high stereoselectivity if the C2-alkoxide could sterically and/or electronically block one face of the oxocarbenium ion-pair intermediate. While there is a wealth of literature devoted to describing the influence of nucleophiles, electrophiles, and reaction conditions in promoting S_N1 and S_N2 manifolds in glycosylation[11,12] and solvolysis[12,13] reactions, at benzylic positions[14,15] and at acetals,[16] the majority of these studies have involved *inter*molecular reactions of relatively simple substrates. Moreover, attempts to distinguish between S_N1 and S_N2 manifolds are complicated by the fact that some of the reactions cited above fall into a gray area along the S_N1–S_N2 continuum and, in some cases, are described as having concurrent, competing reaction manifolds.[15,17,18] We envisioned that detailed kinetic studies of a series of electronically-tuned glycal epoxide substrates would allow us to distinguish between these two pathways in this *intra*molecular reaction of these complex substrates.

Selection of Reaction Probes.

We recently developed a systematic approach to the synthesis of benzannulated spiroketals from C1-aryl glycal substrates.[6] To probe the mechanism of the epoxide-opening spirocyclization, we synthesized a series of these glycal substrates in which the electronic character of the anomeric carbon was modulated using various C1-aryl substituents (Table 1, **5–7**). These substrates were converted to the corresponding glycal epoxides *in situ* and exposed to spontaneous thermal or MeOH-induced spirocyclization conditions.

Diastereomeric product ratios resulting from spontaneous thermal spirocyclizations (−78°C → rt) were first determined to assess the electronic influence of the various aryl substituents (Table 1). While most of these reactions favored spirocyclization with retention of configuration at the anomeric carbon to form thermodynamically-favored (bisanomeric) spiroketals (**11–13**), increasing formation of the contrathermodynamic (mono-anomeric) inversion products (**8–10**) was observed for more electron-deficient substituents (*e.g.*, **5a**–**7a** vs. **5f**–**7f**). These results are as expected for formation of retention products via a presumed S_N1 mechanism, which is favored by electron-donating substituents that stabilize the discrete oxocarbenium intermediate and disfavored by electron-withdrawing substituents that destabilize this intermediate.[19] Interestingly, larger ring systems showed enhanced preferences for spirocyclization with retention of configuration (**5** vs. **6** vs. **7**), suggesting that the corresponding inversion products are formed, at least in part, via an S_N2 mechanism, which becomes less competitive with the S_N1 process as the rate of cyclization decreases, since the rate-limiting step in the latter reaction is oxocarbenium formation rather than cyclization.

Next, we investigated the corresponding MeOH-induced epoxide-opening spirocyclizations (Table 2). As expected, MeOH provided increased selectivity for inversion of configuration compared to the spontaneous thermal spirocyclizations (*cf.* Table 1), although inherent substrate biases could still be observed (*e.g.*, **5a–7a** vs. **5f–7f**). As the methyl glycosides have previously been eliminated as intermediates in these reactions[5] (*e.g.*, double inversion, net retention), the retention products must form via an S_N1 mechanism. Consistent with this mechanism, electron-donating substituents again trended toward increased levels of retention products when considered across the entire substrate panel, presumably by stabilizing the oxocarbenium intermediate, while electron-withdrawing substituents conversely trended toward enhanced selectivity for inversion of configuration by

destabilizing this intermediate. Larger ring systems likewise exhibited enhanced preferences for spirocyclization with retention of configuration (**5** vs. **6** vs. **7**), as well as increased formation of methyl glycoside side products (**16**) that result from competing intermolecular epoxide opening by MeOH, also with retention of configuration at the anomeric carbon. This again suggests that the inversion products are formed preferentially via an S_N2 mechanism that becomes less competitive with alternative S_N1 processes as the rate of cyclization decreases. Notably, the combination of electron-withdrawing substituents and MeOH-induced spirocyclization allowed selective access to 7-membered ring products with inversion of configuration (**10d–f**) for the first time via this approach.[6]

Based on these results, we surmised that this panel of C1-aryl glycal substrates possessed sufficient electronic variability to influence product distribution and to allow us to probe the mechanism of the MeOH-induced epoxide-opening spirocyclization reaction through detailed kinetic studies.

Temperature Dependence of MeOH-Catalyzed Epoxide-Opening Spirocyclization.

Next, in preparation for kinetic studies using low-temperature NMR, we sought to determine the temperature at which epoxide-opening spirocyclization occurs. To provide a direct comparison to our earlier mechanistic studies with the aliphatic glycal **17**,[5] we began by investigating the spirocyclization of this substrate (Table 3). The glycal was dissolved in CD_3OD (17.8 M solvent concentration) and cooled to −78 °C, followed by addition of DMDO in acetone to generate the corresponding glycal epoxide *in situ*. The sample was then transferred to a precooled NMR probe, by which time the glycal had been converted completely to the corresponding glycal epoxide (<3 min). As observed by low-temperature NMR, the glycal epoxide intermediate was stable at −63 °C over a 2 h time frame (entry 1). Conversion to products within 2 h was observed beginning at −40 °C (not shown), with efficient formation of spiroketal **18** and methyl glycoside **20** occurring at −35 °C (entry 2).[20]

In our initial report, we noted that decreased MeOH concentration led to marked decreases in both stereoselectivity (**18** vs. **19**) and chemoselectivity (**18**, **19** vs. **20**).[5] However, consistent with the enhanced selectivities observed with five-membered ring systems above (Tables 1 and 2), stereo- and chemoselective spirocyclization of the glycal epoxide derived from C1-aryl glycal **5c** could be achieved equally effectively at both the original concentration (17.8 M CD_3OD) and a somewhat lower concentration (11.9 M CD_3OD) (entries 3 and 4). Importantly, the glycal epoxide was unreactive at −35 °C in the absence of CD_3OD (entry 5). These findings were valuable as they allowed the convenient design of experiments in which the concentrations of all three solvents could be varied to assess their influences upon reaction outcome and in which the slower reaction rate at 11.9 M CD_3OD facilitated kinetic studies by low-temperature NMR (*vide infra*).

The corresponding six- and seven-membered ring systems (**6c**, **7c**) only began to spirocyclize at higher temperatures and did so with decreased stereo- and chemoselectivity (entries 6 and 7). Consistent with our mechanistic hypotheses above, we reasoned that, for these larger rings, epoxide-opening spirocyclization with inversion of configuration via an S_N2 manifold requires temperatures at which S_N1 reactions via oxocarbenium intermediates become competitive or even dominant.

Thus, having identified appropriate temperatures for NMR analysis of the epoxide-opening spirocyclization reactions, we were poised to carry out detailed kinetic studies of these reactions.

Hammett Analysis of Acid-Catalyzed Spiroketal Epimerization via an S_N1 Mechanism.

Substrates having electron-withdrawing C1-aryl substituents exhibit increased preferences for epoxide-opening spirocyclization with inversion of configuration (Tables 1 and 2). Because oxocarbenium formation should be strongly disfavored in these substrates, we postulated that the inversion products are formed via an S_N2 pathway rather than an S_N1 pathway (Figure 2). To explore this idea further, we first characterized reactions known to proceed by an S_N1 mechanism to serve as a benchmark against which to compare our proposed S_N2 MeOH-catalyzed epoxide-opening spirocyclization.[15,18]

Thus, contrathermodynamic (inversion) spiroketals **8a–f** were treated with TsOH (10 mol% in $CDCl_3$) at rt to induce epimerization to the corresponding thermodynamic (retention) spiroketals **11a–f** via oxocarbenium intermediates **21a–f** (Figure 3a). The rate of conversion via this S_N1 mechanism was measured by NMR. Substrates having electron-donating C1-aryl substituents that stabilize the requisite oxocarbenium intermediate were expected to exhibit faster reaction rates, while substrates having electron-withdrawing substituents were expected to display slower rates. Accordingly, the *p*-methoxy-substituted spiroketal **8a** reacted completely within <2.5 min (Figure 3b), while the *p*-nitro-substituted spiroketal **8f** showed no conversion over 72 h. Spiroketals **8b**–**e**, bearing substituents with intermediate electronic properties, displayed intermediate rates.

Rate constants were determined using the initial rates for these S_N1 processes, and the logarithms of these observed rate constants were plotted against reported σ values to define the Hammett correlation (Figure 3c).[21] Generally, Hammett ρ values range from +5 to −5,[22] with greater absolute values associated with greater buildup of charge at the reactive center. We anticipated that a positive charge would develop at the anomeric center in these reactions, narrowing the range of ρ values to between 0 and approximately −5.[23] As expected, a linear relationship with a ρ value (slope) of −5.1 indicated a distinctly positive S_N1 transition state.

Hammett Analysis of MeOH-Catalyzed Epoxide-Opening Spirocyclization via a Proposed S_N2 Mechanism.

We next used the analogous analysis to probe the transition state for the MeOH-catalyzed epoxide-opening spirocyclization with inversion of configuration (Figure 4a). If an S_N2 mechanism is operative (Figure 2, pathway A), the ρ value should be closer to zero than that observed for the TsOH epimerization above. In contrast, if the epoxide-opening spirocyclization occurs via an S_N1 mechanism involving a discrete oxocarbenium intermediate (Figure 2, pathway B), the ρ value should be similar to that of the TsOH epimerization.

Thus, CD_3OD-catalyzed spirocyclization with inversion of configuration of the glycal epoxides **22a–f** generated *in situ* from **5a–f** (−78 °C, 10 min) was monitored in 11.9 M CD_3OD at −35 °C by NMR (Figure 4b). Rate constants were again determined using the method of initial rates, and the logarithms of the observed rate constants were plotted against reported σ values (Figure 4c).[21] The resulting Hammett correlation exhibited a negative slope with a ρ value of −1.3, consistent with an S_N2 (or S_N2-like) transition state.[14f,15c,d,18,24] The slope was significantly shallower than that observed for the S_N1 process above (ρ = −5.1), indicating the smaller electronic influence of the aryl substituents upon this S_N2 reaction.

Kinetic Analysis of MeOH-Catalyzed Epoxide-Opening Spirocyclization.

To assess the role of MeOH in hydrogen-bonding catalysis of the epoxide-opening spirocyclization with inversion of configuration, we determined the kinetic order of MeOH

in the transition state. Thus, the initial rates of spirocyclization of the glycal epoxide **22c** (R = H) derived *in situ* from glycal **5c** (R = H) were measured in the presence of varying CD_3OD concentrations at −35 °C by NMR.[25] A polynomial curve was obtained, suggesting more than one equivalent of MeOH in the transition state (Figure 5a). Non-linear least squares fit of the data to the equation $f(x) = c[x]^n$ gave values of $c = 6.1\times10^{-5}$ and $n = 2.1$, consistent with second-order catalysis by MeOH. Indeed, plotting the observed rate against $[CD_3OD]^2$ yielded a linear fit with $r^2 = 0.96$ (Figure 5b).

Based on these data, we envision three possible transition states (Figure 6). In transition state **23**, one molecule of MeOH interacts with the epoxide oxygen and another with the attacking nucleophilic alcohol by hydrogen-bonding interactions. In transition state **24**, one MeOH again interacts with the epoxide oxygen, while the second MeOH engages in two hydrogen bonds to both the alcohol nucleophile and the tetrahydropyran ring oxygen. In this model, the second MeOH may direct the nucleophile to *anti*-attack and also enhance reaction selectivity by disfavoring oxocarbenium formation in competing S_N1 pathways. In transition state **25**, both MeOH molecules participate in hydrogen-bonding activation of the epoxide leaving group. This transition state mimics the active site mechanism proposed in epoxide hydrolase enzymes.[26,27]

Strikingly, Jamison and coworkers have also reported second-order catalysis by water in their studies of regioselective epoxide-opening cascades to generate ladder polyethers, and have proposed related hydrogen-bonding interactions in their systems.[9a,b]

Role of the Glycal Ring Oxygen in MeOH-Catalyzed Epoxide-Opening Spirocyclization.

One of the proposed transition states for the MeOH-catalyzed epoxide-opening spirocyclization invokes hydrogen bonding between the glycal ring oxygen and one molecule of MeOH (**24**, Figure 6). This proposal is attractive in that this interaction might also disfavor competing oxocarbenium formation leading to alternative S_N1 pathways. Thus, to investigate the possible role of this glycal ring oxygen, we explored an analogous carbocyclic system lacking that ring oxygen (Figure 7). As expected, the cyclohexene substrate **26** was less reactive to DMDO oxidation, requiring much higher temperature and longer reaction time than the analogous glycals. Moreover, the resulting cyclohexene oxide intermediate **27** could be isolated at rt, facilitating the introduction of other solvents prior to the subsequent spirocyclization step.

Spirocyclization of **27** in neat MeOH (24.6 M) required warming to 60 °C and 24 h reaction time, affording the spiroether **28** with inversion of configuration. Reaction in toluene-d_8 required even higher temperature and longer reaction time (110 °C, 72 h, 85% conversion), establishing the catalytic activity of MeOH in this reaction. Interestingly, treatment of epoxide **27** with TsOH led to rapid conversion to spiroether **28**, again with inversion of configuration, despite the presumably contrathermodynamic nature of this product (axial aryl group observed by NMR).[25] That epoxide opening occurs with inversion of configuration even with TsOH further emphasizes the differences in reactivity between alkyl epoxides such as **27** and those studied previously by Jamison and coworkers,[9] and the corresponding glycal epoxides that are the focus of this study (*cf*. Figure 3), for which stereoselectivity becomes a key consideration due to the electronic influence of the glycal ring oxygen.

We next determined the kinetic order of MeOH in the transition state of the spirocyclization of cyclohexene oxide **27** to spiroether **28** (Figure 8a), for comparison to our results with the analogous glycal epoxide **22c**. Initial rates of spirocyclization were measured in the presence of varying CD_3OD concentrations at 60 °C by NMR (Figure 8b). There was no reaction in neat toluene ($[CD_3OD] = 0$) at 60 °C over the timescale of these experiments. Intriguingly,

fitting the data to $f(x) = c[x]^n$ gave values of $c = 1.8\times10^{-2}$ and $n = 0.59$, indicative of fractional-order kinetics. Indeed, plotting the observed rate against $[CD_3OD]^{0.59}$ yielded a linear fit with $r^2 = 0.99$ (Figure 8c). Fractional orders often suggest a complex kinetic scenario.[28]

Importantly, this result clearly demonstrates that the glycal ring oxygen, while not required for MeOH catalysis in general, is required for second-order catalysis of the epoxide-opening spirocyclization reaction. This may also be considered additional circumstantial support for proposed transition state **24** (Figure 6), which is the only one of the three structures that invokes a specific interaction with the ring oxygen, although removal of the ring oxygen also clearly results in a drastic decrease in the inherent reactivity of the epoxide electrophile, which could certainly cause the change in mechanism. In addition, it remains a formal possibility that subtle steric or conformational changes resulting from replacement of the ring oxygen with a methylene group could also disable either of the other proposed transition states **23** or **25**.

Inhibition of MeOH-Catalyzed Epoxide-Opening Spirocyclization by Acetone.

The *in situ* DMDO epoxidations of the glycal substrates are carried out at −78 °C, a temperature at which spirocyclization does not occur (Table 3), making this step insignificant in our kinetic analyses. However, this step necessarily introduces acetone into the reaction milieu, which remains present during the epoxide-opening spirocyclization reaction.[29] Under our typical reaction conditions, acetone is maximally one-seventh of the total reaction volume (1.9 M), a relatively minor component. Nonetheless, since acetone is both a hydrogen-bond acceptor and an electrophile that may react with MeOH, it is possible that this cosolvent could affect the spirocyclization reaction. Indeed, initial studies indicated that increased relative acetone concentrations led to increased methyl glycoside formation and decreased stereoselectivity.[5,30]

Thus, to determine the potential role of acetone in the spirocyclization reaction, initial rates of spirocyclization of the glycal epoxide **22c** (R = H) derived *in situ* from glycal **5c** (R = H) were measured in the presence of varying acetone concentrations and constant CD_3OD concentration (11.9 M) at −35 °C by NMR.[31] An inhibitory curve was obtained when the rate of spirocyclization was plotted as a function of acetone concentration (Figure 9a). Fitting the data to $f(x) = c[x]^n$ gave values of $c = 2.2\times10^{-2}$ and $n = -1.0$, indicative of first-order inhibition. Indeed, plotting the observed rate against $[\text{acetone}]^{-1}$ yielded a linear fit with $r^2 = 0.99$ (Figure 9b).

The inhibitory activity of acetone suggests that it may sequester MeOH catalyst molecules, lowering the effective concentration of MeOH, leading to a lower rate of spirocyclization and decreased stereoselectivity for inversion of configuration. However, simple subtraction of [acetone] from [MeOH] is insufficient to explain the rate decreases observed in Figure 9. This suggests that complex solvent interactions are involved, in which acetone alters the catalytic activity of MeOH in a non-linear fashion. Indeed, previous experimental and computational studies have shown that the hydrogen-bonded network of MeOH species in neat MeOH is both complex and significantly reorganized by the addition of a hydrogen-bond acceptor such as acetone.[32] Within the range of acetone concentrations examined herein, reorganizations have been described that decrease higher-order MeOH branching off of hydrogen-bonded MeOH chains. Thus, higher concentrations of acetone may disfavor related higher-order MeOH hydrogen-bonding interactions required in the transition state necessary for selective epoxide opening (*cf*. **24**, **25**, Figure 6).

Additionally, the previously observed increase in competing methyl glycoside formation[5,30] in the presence of increased acetone concentrations suggests that this side reaction becomes more competitive at lower effective concentrations of MeOH (*vide infra*).

Competing Intermolecular Methyl Glycoside Formation.

Intermolecular addition of MeOH is a side reaction that can be competitive with the desired epoxide-opening spirocyclization. In our initial studies, we found that, paradoxically, decreased MeOH concentration led to a profound increase in this competing side reaction.[5] As noted above, increased acetone concentrations also lead to increased methyl glycoside formation.[5,30] To understand these effects, we carried out kinetic analysis of the methyl glycoside formation reaction using a substrate that cannot undergo spirocyclization.

Thus, the primary alcohol functionality of glycal **5c** (R = H) was protected as a TBS ether in **29** (Figure 10a). This glycal was then epoxidized with DMDO (−78 °C, 10 min) and initial rates of methyl glycoside formation were measured in the presence of varying CD_3OD concentrations at 15 °C by NMR. Notably, this intermolecular reaction requires a much higher temperature than the corresponding intramolecular spirocyclization, which occurs at −35 °C (*cf*. Table 3). Fitting the data to $f(x) = c[x]^n$ gave values of $c = 1.3\times10^{-3}$ and $n = 1.0$, indicative of first-order dependence of the methyl glycoside formation reaction upon methanol, and plotting the observed rate against $[CD_3OD]$ yielded a linear fit with $r^2 = 0.94$.

We also observed that the methyl glycoside **30** is formed with retention of configuration at the anomeric carbon.[33] At this elevated temperature of 15 °C, we posit that the reaction occurs via an S_N1 mechanism, involving initial methanol-catalyzed epoxide opening to an oxocarbenium intermediate **32** in the rate-limiting step,[34] followed by stereoelectronically favored axial attack of methanol (Figure 11).

Based on these results, it is evident that decreased MeOH concentrations lead to increased methyl glycoside formation by decreasing the *relative* rate of the desired spirocyclization, as the intermolecular reaction is first-order dependent upon MeOH while the intramolecular reaction is second-order dependent upon MeOH. This is, perhaps, not surprising, as an intermolecular reaction via any of the proposed S_N2 transition states (Figure 6) would require *three* molecules of methanol, with third-order dependence likely rendering that reaction manifold kinetically inaccessible. These results are also consistent with the increased methyl glycoside formation observed in the presence of increased acetone concentrations above, whereby acetone lowers the effective concentration of MeOH, increasing the relative rate of the intermolecular reaction compared to the intramolecular reaction.

Interestingly, in their studies of regioselective epoxide-opening cascades, Jamison and coworkers have reported that differential kinetic orders of dependence upon water similarly influence the relative rates of competing *endo* and *exo* reaction manifolds, playing a critical role in the regioselectivity of those reactions.[9b]

Finally, the fact that a single equivalent of MeOH is sufficient to catalyze epoxide opening in the intermolecular S_N1 manifold suggests that only one such hydrogen-bonding interaction is likewise required in the S_N2 epoxide-opening spirocyclization reaction, in contrast to alternative bidentate activation mechanisms precedented in epoxide hydrolase enzymes (**23**,**24** vs. **25**, Figure 6).

CONCLUSION

We have obtained intriguing mechanistic details about the stereoselective MeOH-catalyzed epoxide-opening spirocyclization of glycal epoxides through low-temperature NMR studies of substituted C1-aryl substrates. Hammett analyses of reaction kinetics are consistent with spirocyclization via an S_N2 or S_N2-like mechanism ($\rho = -1.3$ vs. $\rho = -5.1$ for S_N1 reactions of these substrates), leading to inversion of configuration at the anomeric carbon. Additional support for an S_N2 mechanism is provided by the trend toward enhanced stereoselectivity for inversion of configuration observed with electron-deficient substrates that disfavor oxocarbenium formation in competing S_N1 mechanisms. The reaction exhibits second-order dependence on MeOH, with hydrogen-bonding interactions between the substrate and two molecules of MeOH proposed in the spirocyclization transition state (Figure 6). Notably, the glycal ring oxygen is required for second-order MeOH catalysis. Conversely, acetone cosolvent acts as a first-order inhibitor of the reaction, presumably reducing the effective concentration of MeOH by altering its hydrogen-bonding activity. The previous paradoxical finding that decreased MeOH concentrations lead to increased competing intermolecular methyl glycoside formation is resolved by the determination that this side reaction is only first-order dependent on MeOH, proceeding via a presumed S_N1 mechanism. Taken together, the results support a proposed transition state **24**, in which one molecule of MeOH activates the epoxide oxygen while the second chelates both the incoming nucleophile and the glycal ring oxygen to disfavor oxocarbenium formation and possibly to direct *anti* attack.

In our initial report, we noted that other alcohols (EtOH, *i*-PrOH, CF_3CH_2OH, $[CF_3]_2CHOH$) proved to be inferior catalysts in this epoxide-opening spirocyclization reaction with respect to stereo- and/or chemoselectivity.[5] It is apparent that numerous features make MeOH an optimal catalyst for this reaction, including appropriate hydrogen-bonding strength, low acidity, low freezing point, small steric size, low cost, and volatility to facilitate product recovery. While water could theoretically also be an effective catalyst,[9] its use in this reaction is precluded by its higher freezing point, as the glycal epoxides undergo spontaneous thermal spirocyclization even at temperatures below 0 °C (Table 3).

Overall, these studies provide fundamental new insights into the dramatic, specific roles that simple solvents such as MeOH and acetone can play in hydrogen-bonding catalysis and inhibition of stereoselective epoxide-opening reactions of complex molecules. In these systems, MeOH plays a critical role both in providing stereoselectivity (S_N2 vs. S_N1) and in discriminating between competing reaction manifolds (intra- vs. intermolecular). The resulting spiroketal products represent key structural motifs in a wide range of natural products, and MeOH catalysis provides stereocontrolled access to contrathermodynamic spiroketals that are not readily accessible using other synthetic methods. Further, these findings raise the possibility that specific solvent catalysis may be an underappreciated factor in other reactions as well.

Supplementary Material

Refer to Web version on PubMed Central for supplementary material.

Acknowledgments

Dedicated to the memory of our colleague and mentor, Prof. David Y. Gin (1967–2011), with our gratitude for his thoughtful guidance, steadfast support, and invaluable insights into this project. We thank Prof. Dale Drueckhammer (Stony Brook) and Prof. Minkui Luo (MSKCC) for helpful discussions and Dr. George Sukenick, Dr. Hui Liu, Hui Fang, and Dr. Sylvi Rusli for expert NMR and mass spectral support. D.S.T. is an Alfred P. Sloan

Research Fellow. Financial support from the NIH (P41 GM076267), Tri-Institutional Stem Cell Initiative, and Starr Cancer Consortium is gratefully acknowledged.

REFERENCES

(1). (a) Schreiner PR. Chem. Soc. Rev. 2003; 32:289–296. [PubMed: 14518182] (b) Taylor MS, Jacobsen EN. Angew. Chem. Intl. Ed. 2006; 45:1520–1543.

(2). (a) Wassermann A. J. Chem. Soc. 1942:618–621.(b) Yates P, Eaton P. J. Am. Chem. Soc. 1960; 82:4436–4437.

(3). Hine J, Linden S-M, Kanagasabapathy VM. J. Org. Chem. 1985; 50:5096–5099.

(4). (a) Rink R, Kingma J, Spelberg JHL, Janssen DB. Biochemistry. 2000; 39:5600–5613. [PubMed: 10820034] (b) Yamada T, Morisseau C, Maxwell JE, Argiriadi MA, Christianson DW, Hammock BD. J. Biol. Chem. 2000; 275:23082–23088. [PubMed: 10806198]

(5). Potuzak JS, Moilanen SB, Tan DS. J. Am. Chem. Soc. 2005; 127:13796–13797. [PubMed: 16201793]

(6). Liu G, Wurst JM, Tan DS. Org. Lett. 2009; 11:3670–3673. [PubMed: 19634891]

(7). Moilanen SB, Potuzak JS, Tan DS. J. Am. Chem. Soc. 2006; 128:1792–1793. [PubMed: 16464069]

(8). (a) Aho JE, Pihko PM, Rissa TK. Chem. Rev. 2005; 105:4406–4440. [PubMed: 16351049] (b) Perron F, Albizati KF. Chem. Rev. 1989; 89:1617–1661.

(9). (a) Vilotijevic I, Jamison TF. Science. 2007; 317:1189–1192. [PubMed: 17761875] (b) Byers JA, Jamison TF. J. Am. Chem. Soc. 2009; 131:6383–6385. [PubMed: 19385615] (c) Morten CJ, Jamison TF. J. Am. Chem. Soc. 2009; 131:6678–6679. [PubMed: 19402635] (d) Morten CJ, Byers JA, Jamison TF. J. Am. Chem. Soc. 2011; 133:1902–1908.

(10). Lotesta S, Kiren S, Sauers R, Williams L. Angew. Chem. Intl. Ed. 2007; 46:7108–7111.

(11). (a) Lemieux RU, Hendriks KB, Stick RV, James K. J. Am. Chem. Soc. 1975; 97:4056–4062.(b) Banait NS, Jencks WP. J. Am. Chem. Soc. 1991; 113:7951–7958.(c) Nukada T, Berces A, Zgierski MZ, Whitfield DM. J. Am. Chem. Soc. 1998; 120:13291–13295.(d) Jung K–H, Müller M, Schmidt RR. Chem. Rev. 2000; 100:4423–4442. 4442. [PubMed: 11749353] (e) Garcia BA, Gin DY. J. Am. Chem. Soc. 2000; 122:4269–4279.(f) Bérces A, Enright G, Nukada T, Whitfield DM. J. Am. Chem. Soc. 2001; 123:5460–5464. [PubMed: 11389627] (g) Jensen KJ. J. Chem. Soc., Perkin Trans. 1. 2002:2219–2233.(h) Crich D, Chandrasekera NS. Angew. Chem. Intl. Ed. 2004; 43:5386–5389.(i) Kim J-H, Yang H, Park J, Boons G-J. J. Am. Chem. Soc. 2005; 127:12090–12097. [PubMed: 16117550] (j) El-Badri MH, Willenbring D, Tantillo DJ, Gervay-Hague J. J. Org. Chem. 2007; 72:4663–4672. [PubMed: 17539683] (k) Zhu X, Schmidt R. Angew. Chem. Intl. Ed. 2009; 48:1900–1934.(l) Mydock LK, Demchenko AV. Org. Biomol. Chem. 2010; 8:497–510. [PubMed: 20090962]

(12). (a) Piszkiewicz D, Bruice TC. J. Am. Chem. Soc. 1967; 89:6237–6243.(b) Piszkiewicz D, Bruice TC. J. Am. Chem. Soc. 1968; 90:2156–2163. [PubMed: 5644189] (c) Sinnott ML, Jencks WP. J. Am. Chem. Soc. 1980; 102:2026–2032.(d) Namchuk MN, McCarter JD, Becalski A, Andrews T, Withers SG. J. Am. Chem. Soc. 2000; 122:1270–1277.(e) Stubbs JM, Marx D. J. Am. Chem. Soc. 2003; 125:10960–10962. [PubMed: 12952477] (f) Beaver MG, Woerpel KA. J. Org. Chem. 2010; 75:1107–1118. [PubMed: 20108907]

(13). (a) Winstein S, Grunwald E, Jones HW. J. Am. Chem. Soc. 1950; 73:2700–2707.(b) Frisone GJ, Thornton ER. J. Am. Chem. Soc. 1968; 90:1211–1215.(c) Bentley TW, Schleyer P. v. R. J. Am. Chem. Soc. 1976; 98:7658–7666.(d) Arnett EM, Petro C, Schleyer P. v. R. J. Am. Chem. Soc. 1979; 101:522–526.(e) Koo IS, An SK, Yang K, Lee I, Bentley TW. J. Phys. Org. Chem. 2002; 15:758–764.

(14). (a) Baker JW. J. Chem. Soc. 1933:1128–1133.(b) Baker JW, Nathan WS. J. Chem. Soc. 1935:519–527.(c) Baker JW, Nathan WS. J. Chem. Soc. 1935:1840–1844.(d) Sugden W, Willis JB. J. Chem. Soc. 1951:1360–1363.(e) Amyes TL, Richard JP. J. Am. Chem. Soc. 1990; 112:9507–9512.(f) Buckley N, Oppenheimer NJ. J. Org. Chem. 1996; 61:7360–7372. [PubMed: 11667662] (g) Toteva MM, Richard JP. J. Am. Chem. Soc. 2002; 124:9798–9805. [PubMed: 12175239]

(15). (a) Richard JP, Jencks WP. J. Am. Chem. Soc. 1982; 104:4689–4691.(b) Richard JP, Jencks WP. J. Am. Chem. Soc. 1982; 104:4691–4692.(c) Lim C, Kim S–H, Yoh S–D, Fujio M, Tsuno Y. Tetrahedron Lett. 1997; 38:3243–3246.(d) Yoh SD, Cheong DY, Lee CH, Kim SH, Park JH, Fujio M, Tsuno Y. J. Phys. Org. Chem. 2001; 14:123–130.

(16). (a) Young PR, Jencks WP. J. Am. Chem. Soc. 1977; 99:8238–8248.(b) Amyes TL, Jencks WP. J. Am. Chem. Soc. 1989; 111:7900–7909.(c) Buckley N, Oppenheimer NJ. J. Org. Chem. 1996; 61:8048–8062. [PubMed: 11667788] (d) Liras JL, Lynch VM, Anslyn EV. J. Am. Chem. Soc. 1997; 119:8191–8200.(e) Shenoy SR, Woerpel KA. Org. Lett. 2005; 7:1157–1160. [PubMed: 15760163] (f) Krumper JR, Salamant WA, Woerpel KA. Org. Lett. 2008; 10:4907–4910. [PubMed: 18844363] (g) Krumper JR, Salamant WA, Woerpel KA. J. Org. Chem. 2009; 74:8039–8050. [PubMed: 19813702]

(17). (a) Gold V. J. Chem. Soc. 1956:4633–4637.(b) Ingold, CK. Structure and Mechanism in Organic Chemistry. 2nd ed.. Cornell University Press; Ithaca, NY: 1969. (c) Bartlett PD. J. Am. Chem. Soc. 1972; 94:2161–2170.(d) Sneen RA. Acc. Chem. Res. 1973; 6:46–53.(e) Jencks WP. Chem. Soc. Rev. 1981; 10:345–375.(f) Katritzky AR, Brycki BE. Chem. Soc. Rev. 1990; 19:83–105.(g) Buckley N, Oppenheimer NJ. J. Org. Chem. 1997; 62:540–551. [PubMed: 11671447] (h) Smith, MB.; March, J. March's Advanced Organic Chemistry. 6th ed.. Wiley; New York: 2007. Chapter 10

(18). Phan TB, Nolte C, Kobayashi S, Ofial AR, Mayr H. J. Am. Chem. Soc. 2009; 131:11392–11401. [PubMed: 19634906]

(19). (a) Jorge JAL, Kiyan NZ, Miyata Y, Miller J. J. Chem. Soc., Perkin Trans. 2. 1981:100–103.(b) Vitullo VP, Grabowski J, Sridharan S. J. Chem. Soc., Chem. Commun. 1981:737–738.

(20). Our original experimental protocol (ref. 5; 92:0:8 ratio of **18:19:20**) called for rapid addition of MeOH to the −63 °C CH_2Cl_2/acetone solution of the glycal epoxide, which likely resulted in transient warming of the reaction mixture to a temperature at which the spirocyclization occurred. The reaction may also have proceeded during warming from −63 °C to rt prior to workup. Along these lines, low-temperature NMR analysis of the reaction during that warming process (−63 °C → rt over 15 min) herein indicated formation of a 80:0:20 ratio of **18:19:20**.

(21). Hansch C, Leo A, Taft RW. Chem. Rev. 1991; 91:165–195.

(22). (a) Hammett LP. J. Am. Chem. Soc. 1937; 59:96–103.(b) Carpenter, BK. Determination of Organic Reaction Mechanisms. Wiley; United States: 1984. Chapter 7

(23). Absolute ρ values between 0 and 1 are usually seen as radical reactions, further narrowing our range of expected Hammett correlation values. (*e.g.*, Pryor WA, Lin TH, Stanley JP, Henderson RW. J. Am. Chem. Soc. 1973; 95:6993–6998.

(24). Interestingly, while there are many precedents for U- or V-shaped curves in Hammett correlations for S_N2 reactions at benzylic centers, the plot had fairly good linearity in this case ($r^2 = 0.92$). Hammett plot curvatures across different substituents have been attributed to changing mechanism from S_N1 to S_N2, changing polarity of the transition state (degree of bond formation vs. cleavage), changing ability to stabilize the transition state based on different inductive and resonance capacities, or changing electrostatic interactions between reaction partners. In this case, the negative ρ value is indicative of positive charge buildup at the reactive center. If the C1-aryl ring is in full conjugation with the reactive center in the transition state, a positive deviation in the left portion of the plot would be expected, indicating enhanced rate acceleration due to resonance effects for the *p*-OMe and *p*-Me substituents. Alternatively, if the C1-aryl ring is fully out of conjugation from the reactive center, as is the case in the spiroketal product, a negative deviation in the left portion of the plot would be expected, due to inductive electron-withdrawing effect of the *p*-OMe substituent. Accordingly, the linear plot observed is suggestive of a transition state in which the aromatic ring is partially conjugated to the reactive center. For lead references on the analysis of S_N2 reactions of benzylic systems, see: (a) Young PR, Jencks WP. J. Am. Chem. Soc. 1979; 101:3288–3294. (b) Galabov B, Nikolova V, Wilke JJ, Schaefer HF, Allen WD. J. Am. Chem. Soc. 2008; 130:9887–9896. [PubMed: 18597451]

(25). See Supporting Information for full details.

(26). Lau EY, Newby ZE, Bruice TC. J. Am. Chem. Soc. 2001; 123:3350–3357. [PubMed: 11457071]

(27). Attempts to distinguish between these possible transition states using computational methods have been unsuccessful thus far.

(28). Smith, MB.; March, J. March's Advanced Organic Chemistry. 6th ed.. Wiley; New York: 2007. Chapter 6

(29). (a) DMDO is prepared from acetone and was delivered herein as an 0.073 M solution in acetone: Murray RW, Jeyaraman R. J. Org. Chem. 1985; 50:2847–2853. (b) Previous efforts in our laboratory to generate acetone-free DMDO using a published protocol have been unsuccessful: Gilbert M, Ferrer M, Sanchez-Baeza F, Messeguer A. Tetrahedron. 1997; 53:8643–8650. (c) In addition, the epoxidation reaction itself produces one equivalent of acetone as a byproduct.

(30). Potuzak, JS. PhD. Dissertation. Cornell University; 2007.

(31). Acetone-d_6 was added prior to treatment with DMDO in acetone-h_6 to achieve higher acetone concentrations in these experiments.

(32). For lead references on MeOH–acetone liquid mixtures, see: (a) Venables DS, Schmuttenmaer CA. J. Chem. Phys. 2000; 113:3249–3260. (b) Max J-J, Chapados C. J. Chem. Phys. 2005; 122:014504/1–18.

(33). Methyl glycosides **16a–e** (*cf*. Table 2) were similarly observed exclusively with retention of configuration at the anomeric carbon. Interestingly, this stereoselectivity in the aryl substrate series is not seen in the aliphatic substrate series, where both glycoside anomers are observed (ref. 5). This may result from the increased steric bulk of the C1-aryl substituent in **30**, further disfavoring an axial orientation.

(34). For a lead reference on glycoside hydrolysis via S_N1 mechanisms, see: Ahmad IA, Birkby SL, Bullen CA, Groves PD, Lankau T, Lee WH, Maskill H, Miatt PC, Meneer ID, Shaw K. J. Phys. Org. Chem. 2004; 17:560–566.

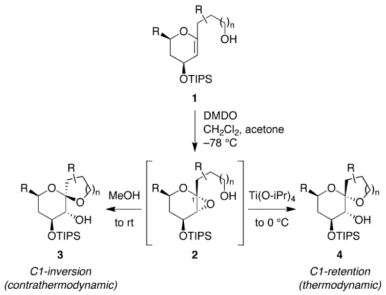

Figure 1.

Stereoselective spirocyclization of glycal epoxides (**2**) with inversion (**3**) or retention (**4**) of configuration at the anomeric carbon. DMDO = dimethyldioxirane; TIPS = triisopropylsilyl.

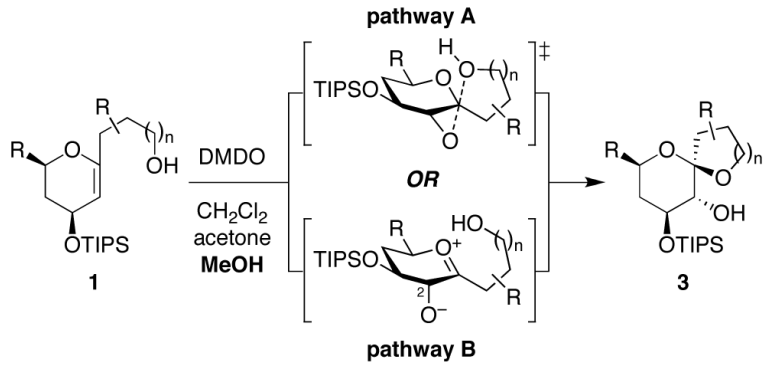

Figure 2.
Possible S_N2 and S_N1 mechanisms for MeOH-induced epoxide-opening spirocyclization of glycal epoxides with inversion of configuration at the anomeric carbon.

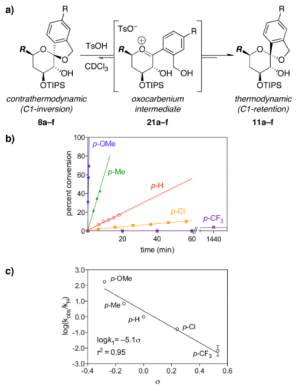

Figure 3.

Hammett analysis of acid-catalyzed spiroketal epimerization via an S_N1 mechanism. a) S_N1 mechanism for acid-catalyzed epimerization of contrathermodynamic (inversion) spiroketals **8a–f** to thermodynamic (retention) spiroketals **11a–f**. ***R*** = $CH_2CH_2OTBDPS$. b) Rates of conversion with 10 mol% TsOH in $CDCl_3$ at rt. The *p*-nitro-substituted substrate **8f** does not react within 72 h under these conditions. Pseudo-first-order rate differences among the six substrates **8a–f** illustrate the electronic requirements for the formation of oxocarbenium intermediates **21a–f**. Representative data from one of two replicate experiments shown. c) Hammett plot exhibits a linear correlation for the electronically varied substrates **8a–e** with a steep negative slope indicative of an S_N1 transition state ($\rho = -5.1$).

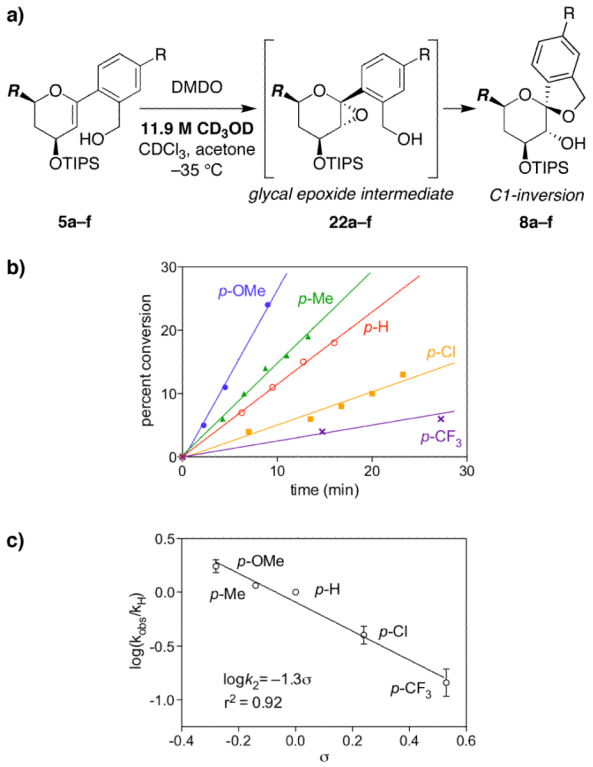

Figure 4.

Hammett analysis of methanol-catalyzed epoxide-opening spirocyclization via a proposed S_N2 mechanism. a) Methanol-catalyzed epoxide-opening spirocyclization of glycal epoxides **22a–f** with inversion of configuration to afford spiroketals **8a–f**. ***R*** = $CH_2CH_2OTBDPS$. b) Rates of inversion product formation with 11.9 M CD_3OD (4:3:1.3 $CD_3OD/CDCl_3$/acetone) at −35 °C. The *p*-methoxy-substituted substrate **5a** also forms the corresponding retention product **11a**, but the diagnostic NMR peaks are resolved. The linear fit for the *p*-CF_3-substituted substrate **5e** is based upon a total of seven datapoints out to 52 min,[25] although only the first three datapoints are shown for clarity. The *p*-nitro-substituted glycal epoxide intermediate **22f** does not react at this temperature. Representative data from one of three replicate experiments shown. c) Hammett plot exhibits a linear correlation for the electronically varied substrates **22a–e** with a shallow negative slope indicative of an S_N2 transition state ($\rho = -1.3$).

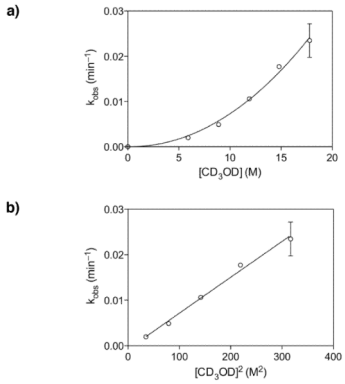

Figure 5.

Second-order catalysis by methanol in the epoxide-opening spirocyclization of glycal epoxide **22c** (R = H). a) Plot of k_{obs} (min^{-1}) for inversion product formation at varying $[CD_3OD]$ yields a polynomial curve. Mean values over two replicate experiments shown. b) Plot of k_{obs} (min^{-1}) versus $[CD_3OD]^2$ yields a linear correlation, consistent with second-order dependence on methanol. Mean values over two replicate experiments shown.

Figure 6.

Three possible S_N2 transition states for MeOH-catalyzed epoxide-opening spirocyclization with inversion of configuration under MeOH hydrogen-bonding catalysis. In transition state **23,** both the epoxide leaving group and alcohol nucleophile are activated with separate MeOH hydrogen bonds. Transition state **24** is similar, but the upper MeOH also engages in a second hydrogen bond to the tetrahydropyran ring oxygen that may disfavor competing S_N1 mechanisms involving oxocarbenium formation. In transition state **25,** the epoxide electrophile is activated by two MeOH hydrogen bonds, as seen in epoxide hydrolase enzymes.[26]

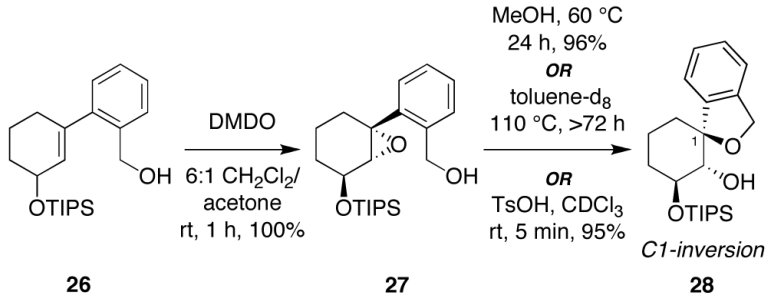

Figure 7.

Epoxide-opening spirocyclizations of a cyclohexene oxide substrate lacking the glycal ring oxygen. The thermal spirocyclization in toluene-d_8 proceeds to only 85% conversion even after 72 h. Stereochemical assignments were determined by ^{1}H-NMR and NOESY analysis of the spiroether product.

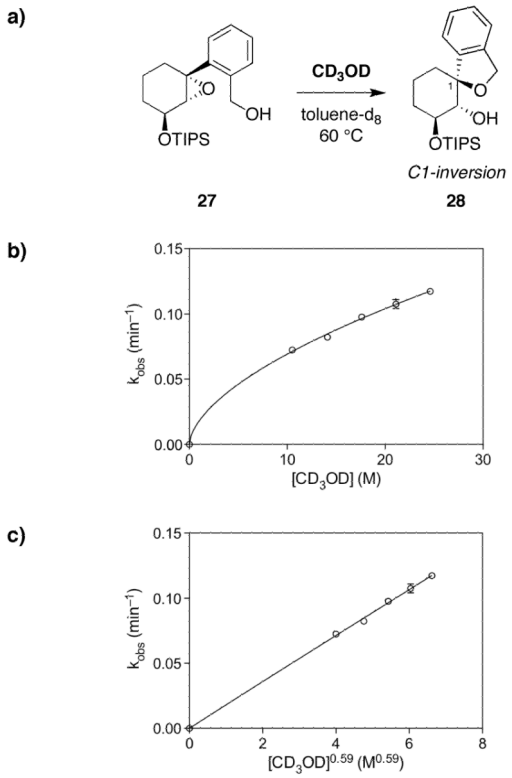

Figure 8.

Fractional-order catalysis by methanol in the epoxide-opening spirocyclization a substrate lacking the glycal ring oxygen. a) Methanol-catalyzed epoxide-opening spirocyclization of cyclohexene oxide **27** with inversion of configuration to afford spiroether **28**. b) Plot of k_{obs} (min^{-1}) for spiroether formation at varying [CD_3OD] yields a fractional-order curve. Mean values over two replicate experiments shown. c) Plot of k_{obs} (min^{-1}) versus $[CD_3OD]^{0.59}$ yields a linear correlation, consistent with the fractional-order dependence on methanol. Mean values over two replicate experiments shown.

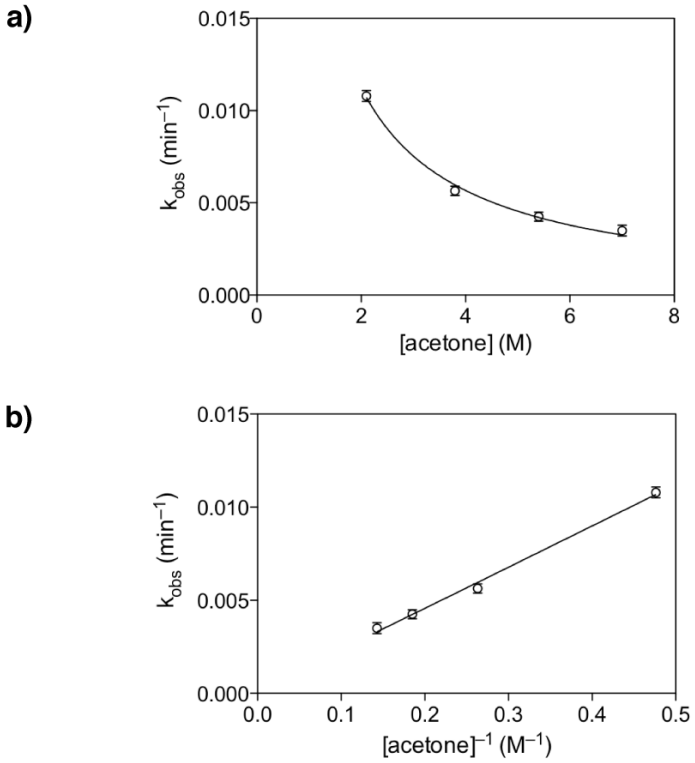

Figure 9.

First-order inhibition by acetone in the epoxide-opening spirocyclization of glycal epoxide **22c** (R = H). a) Plot of k_{obs} (min^{-1}) for inversion product formation at varying [acetone] yields an inhibitory curve. Mean values over two replicate experiments shown. b) Plot of k_{obs} (min^{-1}) versus $[acetone]^{-1}$ yields a linear correlation, consistent with negative first-order dependence on acetone. Mean values over two replicate experiments shown.

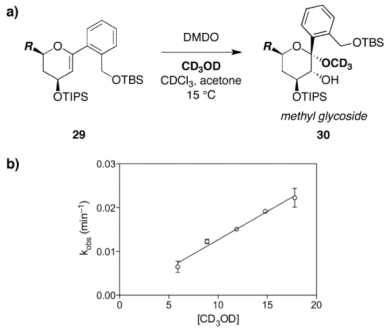

Figure 10.

First-order dependence on methanol in the intermolecular methyl glycoside formation side reaction. a) Methanolysis of the glycal epoxide generated *in situ* from protected glycal **29** to afford methyl glycoside **30**. b) Plot of k_{obs} (min^{-1}) versus [CD_3OD] yields a linear correlation, consistent with first-order dependence on methanol. Mean values over two replicate experiments shown.

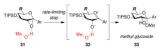

Figure 11.
Proposed S_N1 mechanism for competing intermolecular methyl glycoside-forming side reaction.

Table 1

Spontaneous Thermal Spirocyclizations of Substituted C1-Aryl Glycal Epoxides.[a]

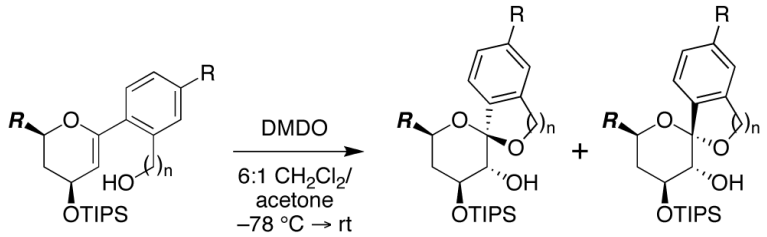

C1-inversion *C1-retention*

5a–f: n = 1
6a–f: n = 2
7a–f: n = 3

8a–f: n = 1
9a–f: n = 2
10a–f: n = 3

11a–f: n = 1
12a–f: n = 2
13a–f: n = 3

ratio of inversion (8–10) to retention (11–13) products						
	R = OMe (a)	**Me (b)**	**H (c)**	**Cl (d)**	**CF_3 (e)**	**NO_2 (f)**
8:11 (n = 1)	<2:98	13:87	31:69	32:68	27:73	67:33
9:12 (n = 2)	<2:98	<2:98	9:91	19:81	43:57	44:56
10:13 (n = 3)	<2:98	<2:98	<2:98	<2:98	<2:98	18:82

R = $CH_2CH_2OTBDPS$.

[a]Glycal epoxides generated in situ from glycal precursors with DMDO (−78 °C, 10 min), then allowed to warm to rt. Reactions proceeded in quantitative yields and product ratios were determined by ^{1}H-NMR analysis.

Table 2

MeOH-Induced Spirocyclizations of Substituted C1-Aryl Glycal Epoxides.[a]

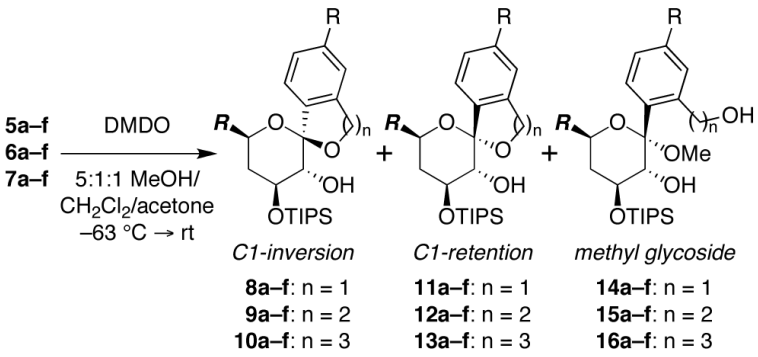

	ratio of inversion (8–10) to retention (11–13) products					
	R = OMe (a)	**Me (b)**	**H (c)**	**Cl (d)**	**CF_3 (e)**	**NO_2 (f)**
8:11 (n = 1)	88:12	95:5	>98:2	>98:2	>98:2	>98:2
9:12 (n = 2)	5:95	37:63	47:53	55:45	68:32	63:37
10:13 (n = 3)	<2:51[b]	<2:46[b]	<2:38[b]	18:44[b]	81:12[b]	93:7

R = $CH_2CH_2OTBDPS$.

[a] Glycal epoxides generated *in situ* from glycal precursors with DMDO (−78 °C, 10 min), stirred at −63 °C for 2 h, then allowed to warm to rt. Reactions proceeded in quantitative yields and product ratios were determined by ^{1}H-NMR analysis.

[b] Remainder methyl glycoside 16.

Table 3

Optimal Temperatures for Stereoselective Epoxide-Opening Spirocyclization of Glycal Epoxide Substrates.[a]

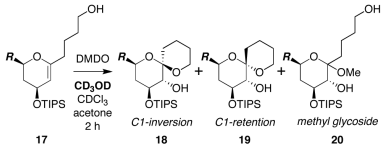

entry	substrate[a]	T (°C)	CD_3OD (M)	inversion (18, 8-10)	retention (19, 11-13)	glycoside (20, 14-16)
1	**17**	−63	17.8[b]		nr	
2	**17**	−35	17.8	93	0	7
3	**5c** (R = H)	−35	17.8	>98	<2	0
4	**5c** (R = H)	−35	11.9[c]	>98	<2	0
5	**5c** (R = H)	−35	0		nr	
6	**6c** (R = H)	−20	17.8	70	30	0
7	**7c** (R = H)	0	17.8	0	41	59

R = $CH_2CH_2OTBDPS$; nr = no reaction.

[a] Glycal epoxides generated *in situ* from glycal precursors with DMDO (−78 °C, 10 min), then warmed to the indicated temperature in the NMR probe.

[b] 6:1:1.3 $CD_3OD/CDCl_3$/acetone.

[c] 4:3:1.3 $CD_3OD/CDCl_3$/acetone.

J Am Chem Soc. Author manuscript; available in PMC 2012 May 25.